Dye-Sensitized Solar Cells

Towards Compatibility between Ruthenium Sensitizers and Cobalt Electrolytes in Dye-Sensitized Solar Cells**

*Lauren E. Polander, Aswani Yella, Basile F. E. Curchod, Negar Ashari Astani, Joël Teuscher, Rosario Scopelliti, Peng Gao, Simon Mathew, Jacques-E. Moser, Ivano Tavernelli, Ursula Rothlisberger, Michael Grätzel, Md. Khaja Nazeeruddin, and Julien Frey**

Dye-sensitized solar cells (DSCs)[1] are low-cost alternatives to conventional silicon technologies for solar energy conversion. A typical DSC is composed of a chromophore that is anchored to a mesostructured anode of anatase titania (TiO$_2$). Upon absorption of photons, electrons are injected from the excited state of the dye into the TiO$_2$ conduction band. Subsequently, the ground state form of the sensitizer is regenerated by reductive electron transfer from the electrolyte. The electrons injected into the semiconductor flow towards the counter electrode where the redox mediator is in turn reduced.[2] Under simulated AM 1.5 G illumination (100 mW cm^{-2}), the power conversion efficiency of a cell (η) is defined as the product of the generated photocurrent density (J_{SC}), the open-circuit photovoltage (V_{OC}),[3] and the fill factor (FF), as follows: $\eta = J_{SC} V_{OC} FF$.[4]

In addition to their long-term stability, sensitizers of the [Ru(2,2′-bipyridine)$_2$(NCS)$_2$] type have attained power conversion efficiencies of up to 12% with iodine electrolytes.[5–9] The recent surge of organic dyes to this level of performance can be largely explained by the development of alternative redox mediators, in particular cobalt(II/III) complexes.[10] In contrast to the iodide/triiodide couple (I$^-$/I$_3^-$), the electrochemical potential of these species can be adjusted through substitution and/or the modification of the ligand skeleton.[11–15] This tuning minimizes energy losses in the device by optimizing the driving force for regeneration, which allows for considerable improvement of the open-circuit voltage relative to iodine electrolytes.

Current ruthenium(II) sensitizers are not designed to perform with cobalt electrolytes. Among the few examples reported in the literature,[11, 16–20] only limited performances have been achieved. The highest performing dye (Z907) yields efficiencies of up to 6.5% with cobalt[18] vs. 8.5% with iodine,[21] unless the coadsorbent is specifically engineered.[22] Molecular dynamic simulations suggest close contact interactions between the cobalt(III) species and the anchored sensitizer(s), which causes undesired recombination of the electrons injected into the TiO$_2$ to the redox mediator.[23] Similar issues have been addressed for organic dyes through the addition of peripheral bulky substituents. This strategy prolongs the electron lifetime in the semiconductor by preventing the electrolyte from accessing the surface.[12]

Implementation of a similar design principle could improve compatibility between ruthenium(II) sensitizers and cobalt electrolytes. Cyclometalated tris-heteroleptic complexes have the desirable photoelectrochemical properties[24] to yield high-efficiency DSCs,[25] while presenting versatility towards NCS-free sensitizers. Herein, we report a design that takes advantage of this multifunctional structure to insulate the surface from the electrolyte, tune the energy levels and the light-harvesting properties of the complex, and provide an anchor to the TiO$_2$. Owing to this rational design, DSCs exhibiting comparable efficiencies with both cobalt and iodine redox mediators were obtained.
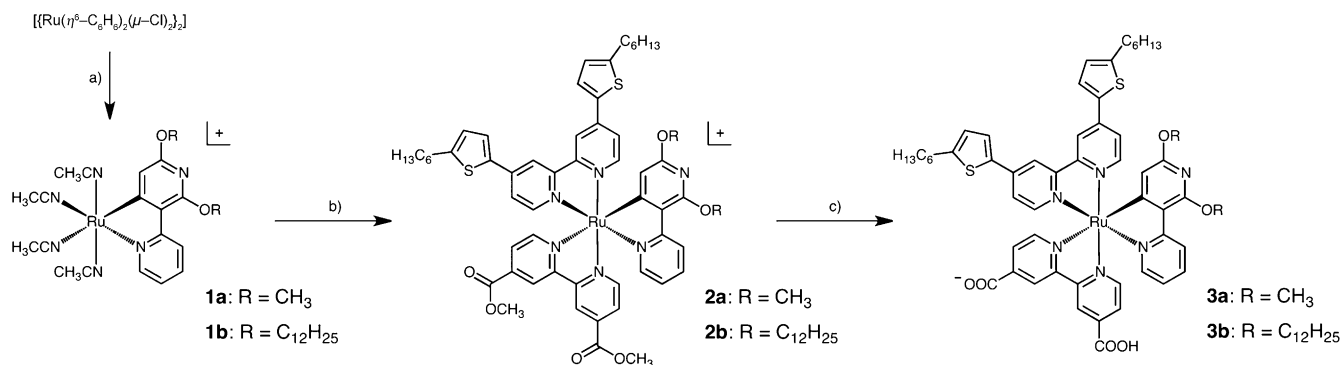
To improve compatibility of ruthenium(II) sensitizers with cobalt redox mediators, one could design a tris-heteroleptic complex that maintains favorable highest occupied molecular orbital (HOMO) energetics while also enabling interfacial control at the TiO$_2$ surface. However, thus far the literature does not contain a ligand that fulfills both of these criteria.[26, 27] We found 2′,6′-dimethoxy-2,3′-bipyridine to be convenient for tuning the HOMO energy level. The alkoxy substituents are also advantageous as a substitution point to insulate the TiO$_2$ surface by elongation of the chains. To validate this concept, both methoxy- and dodecyloxy-derivatives were synthesized. The other two ligands used to complete the coordination sphere of the ruthenium center have two functions: 2,2′-bis(5-hexylthiophen-2-yl)-2,2′-bipyr-

[*] Dr. L. E. Polander, Dr. A. Yella, Dr. J. Teuscher, R. Scopelliti,
Dr. P. Gao, Dr. S. Mathew, Prof. M. Grätzel, Dr. M. K. Nazeeruddin,
Dr. J. Frey
Laboratory of Photonics and Interfaces, Institute of Chemical
Science and Engineering, École Polytechnique Fédérale
de Lausanne, 1015 Lausanne (Switzerland)
E-mail: julien.frey@gmail.com

B. F. E. Curchod, N. Ashari Astani, Dr. I. Tavernelli,
Prof. U. Rothlisberger
Laboratory of Computational Chemistry and Biochemistry, Institute
of Chemical Science and Engineering, École Polytechnique Fédérale
de Lausanne, 1015 Lausanne (Switzerland)

Prof. J.-E. Moser
Group for Photochemical Dynamics, Institute of Chemical Science
and Engineering, École Polytechnique Fédérale de Lausanne
1015 Lausanne (Switzerland)

Scheme 1. Synthesis of complexes **3a** and **3b**. Charged complexes were isolated as PF_6^- salts. a) 2′,6′-dimethoxy-2,3′-bipyridine or 2′,6′-bis(dodecyloxy)-2,3′-bipyridine, NaOH, KPF_6 in MeCN (**1a**: 56%, **1b**: 43%); b) 2,2′-bis(5-hexylthiophen-2-yl)-2,2′-bipyridine, 4,4′-dimethylester-2,2′-bipyridine in EtOH (**2a**: 48%; **2b**: 45%); c) DMF, H_2O, Et_3N (3:1:1) (**3a**: 77%; **3b**: 95%).

idine enhances the absorptivity of the complex, compared to an unsubstituted 2,2′-bipyridine ligand,[7] whereas 2,2′-bipyridine-4,4′-dicarboxylic acid serves as an electron-accepting ligand and anchor to the TiO_2.

Complexes **1–3** were prepared by following a straightforward procedure developed by Berlinguette et al.[19] As shown in Scheme 1, with [{$Ru(C_6H_6)Cl_2$}$_2$] as the ruthenium source, the cyclometalating ligand is introduced first to yield precursors **1a** and **1b**. The complex is subsequently reacted with stoichiometric amounts of the two different bipyridine ligands, in a one-pot procedure that gives the desired complexes, **2a** or **2b**, in yields close to the theoretical limit. Finally, sensitizers **3a** and **3b** are obtained as neutral complexes after saponification. Unlike most ruthenium(II) sensitizers, which are isolated using size-exclusion chromatography, complexes **1–3** can be purified using conventional chromatography over alumina or silica and by using precipitation techniques. Details on the synthesis and characterization of these compounds are given in the Supporting Information.

Owing to their tris-heteroleptic nature, complexes **2** and **3** can potentially adopt two conformations with cyclometalation either in *trans* to the dicarboxy-bipyridine or in *trans* to the dithiophenyl-bipyridine ligand. The NMR data indicate that a single isomer is produced. To confirm the arrangement of the ligands around the metal center, single crystals of **2a** were grown by slow diffusion of hexane into a dichloromethane solution. The crystal structure is shown in Figure 1, with selected bond lengths and angles presented in the Supporting Information, Table S2. As expected, the complex adopts a distorted octahedral geometry around the ruthenium center. The dimethoxy ester bipyridine ligand, located *trans* to the cyclometalated ring, experiences the electron donating character of the C24–Ru bond, which manifests in an elongation of the Ru–N1 bond. The NMR analysis from which we conclude that complexes **2** and **3** adopt this same conformation (Figures S7 and S8) is consistent with the observed *trans* effect, as detailed in the Supporting Information. The methoxy substituents of the cyclometalated ring are arranged within the plane of the ligand to avoid lone pair interactions with the pyridyl nitrogen. At the light-harvesting
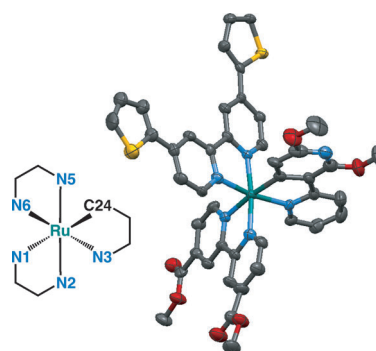

Figure 1. Crystal structure of **2a**·2 CH_2Cl_2. Thermal ellipsoids are drawn at the 50% probability level. The counter ion, hexyl chains, hydrogen atoms, and solvent molecules are omitted for clarity. Additional information can be found in Table S1. N blue, O red, S yellow, Ru turquoise.

ligand, the thiophenes lie in the 2,2′-bipyridine plane (torsions angles < 1°), thus ensuring good electronic communication.

The optical and electrochemical properties of **3a** and **3b** were determined in dichloromethane solution (Figure 2; see also Figures S10 and S11). Both complexes show virtually identical properties, as summarized in Table S3. The UV/Vis spectrum of **3b** shows broad and intense absorptions below 350 nm that are dominated by π–π* transitions. At longer wavelengths, the spectrum reveals two strong bands centered
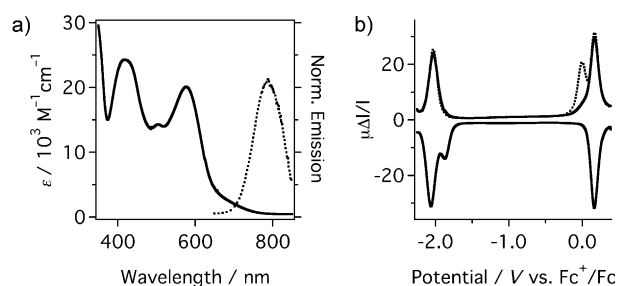

Figure 2. a) Steady-state absorption (——) and normalized emission spectra (-----, λ_{exc} = 580 nm), and b) differential pulse voltammogram (——) with a ferrocene internal standard (-----) in dichloromethane of **3b**. Scan rate of 100 mV s^{-1} with 10 mV pulses.

at 418 nm (23 400 M cm⁻¹) and 580 nm (19 600 M cm⁻¹), which are characteristic of metal-to-ligand charge-transfer transitions. These assignments are further supported by time-dependent density functional theory calculations for **3a** (LR-TDDFT/M06; Figures S12–S21). Full details on the quantum chemical calculations can be found in the Supporting Information.

Furthermore, the energy levels of complexes **3a** and **3b** are adequately poised for use in DSCs. The differential pulse voltammogram of complex **3b** exhibits quasi-reversible one-electron oxidation at $+0.86$ V ($E_{HOMO} = -4.91$ eV) and one-electron reduction at -1.35 V vs. NHE.[28] The anodic peak potential is ascribed to oxidation of the metal center to ruthenium(III), whereas the cathodic peak is assigned to a ligand-centered reduction. According to (U)DFT/M06 calculations, the vertical ionization energy of **3a** is calculated at 5.04 eV, whereas the adiabatic ionization energy lies at 4.96 eV. Both values are in good agreement with the estimated HOMO energy and corroborate the oxidation of the ruthenium center.[29] As observed in Figure S13, the spin density of the geometry optimized **3a**·⁺ appears only slightly delocalized over the cyclometalated pyridine.

These $E_{S+/S}$ values allow regeneration of **3a**·⁺ and **3b**·⁺ from iodine ($E^0 = +0.35$ V vs. NHE), as well as a variety of cobalt-based electrolytes with more positive electrochemical potentials.[13] In this study, a tris(1,10-phenanthroline) cobalt-(II/III) ([Co^{II/III}(phen)_3]^{2/3+}, $E^0 = +0.62$ V vs. NHE) electrolyte is chosen to maximize the V_{OC} while maintaining sufficient driving force for regeneration. The excited state oxidation potential of the dyes ($E_{S+/S*}$) is estimated using the zero–zero transition energy (E_{0-0}) measured at the intersection of the absorption and normalized emission spectra. The $E_{S+/S*}$ values obtained for **3a** and **3b** (ca. -0.90 V vs. NHE) provide a priori ample driving force for electron injection into the TiO₂ conduction band ($E_C = $ ca. -0.5 V vs. NHE).[30]

Provided that electron injection is not an issue, the efficiency of TiO₂ films sensitized with **3a** and **3b** depends on two main charge-transfer reactions: 1) back-recombination, which corresponds to electron transfer from the electron in the TiO₂ to the oxidized dye, and 2) dye-regeneration, which corresponds to reductive electron transfer from the electrolyte to the oxidized sensitizer. Their respective time constants (τ_{rec} and τ_{reg}) can be quantified using transient absorption (TA) decay measurements. The oxidized forms of the dyes have absorption spectra that differ sharply from their neutral counterparts (Figure 3a,b). Following excitation at 470 nm, the photoinduced absorption (PIA) signal that appears at 740 nm is characteristic of the formation of a ruthenium(III) species,[31] whose TA decay is used to derive the corresponding time constants. The decays were fitted with a single exponential component $\Delta A(t) \propto A_0 \exp[-(t/\tau)]$, where A_0 is the pre-exponential factor and τ is the characteristic time constant.[32] The fits are represented as solid lines on Figure 3c,d. With an inert electrolyte, τ_{rec} was estimated at 280 and 373 µs for **3a** and **3b**, respectively. In contrast, the presence of [Co^{II/III}(phen)_3]^{2/3+} gives rise to accelerated TA decays, with τ_{reg} values of 9.7 µs and 17 µs for **3a** and **3b**, respectively. These τ_{rec} and τ_{reg} constants indicate nearly quantitative regeneration quantum yields, $\Phi_{reg} = k_{reg}/$

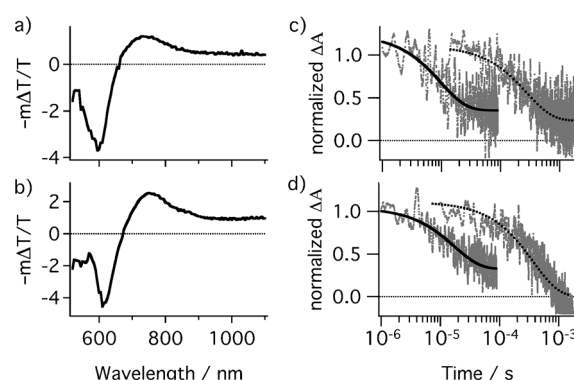**Figure 3.** a,b) PIA spectra after 470 nm excitation, and (c,d) TA decay traces following excitation at 520 nm (probe at 750 nm) of 8.0 µm thick TiO₂ films coated with **3a** (a, c) and **3b** (b, d), respectively. Decays in acetonitrile (•••••) and in presence of [Co^{II/III}(phen)_3]^{2/3+} electrolyte (——) were fitted with a single exponential component $\Delta A(t) \propto A_0 \exp[-(t/\tau)]$. 7 ns (fwhm) laser pulse of 50 µJ cm⁻².

$(k_{reg} + k_{rec}) = 96\%$ (where $k_i = 1/\tau_i$), which is paramount for efficient DSCs.

The incident photon-to-current efficiency (IPCE) spectra using a [Co^{II/III}(phen)_3]^{2/3+} electrolyte are shown in Figure 4a. Complex **3b** was also investigated using I⁻/I₃⁻ for comparison purposes. The three IPCEs have a similar shape in the range
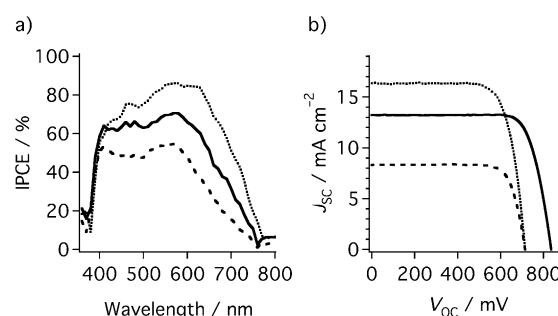
Figure 4. a) Photocurrent action spectra in mesoscopic solar cells, and b) J–V characteristics measured under simulated AM 1.5 G full sun illumination (100 mW cm⁻²) for devices employing **3a** and **3b**. Film thickness: (4.0 + 4.0) µm. Cobalt electrolyte: 0.25 M [Co(phen)_3](TFSI)_2, 0.05 M [Co(phen)_3](TFSI)_3, 0.25 M TBP, 0.1 M LiTFSI in acetonitrile; iodine electrolyte: 1.0 M PMII, 0.03 M I₂, 0.5 M TBP, 0.1 M GuNCS, 0.05 M LiI. **3a**+cobalt (-----), **3b**+cobalt (——), **3b**+iodine (•••••). GuNCS = guanidinium thiocyanate, phen = 1,10-phenanthroline, PMII = 1-propyl-3-methylimidazolium iodide, TBP = 4-*tert*-butylpyridine, TFSI = trifluoromethanesulfonimide.

of 380–770 nm, but with significantly different intensities. Similar to other ruthenium(II) sensitizers,[18,19,22] the photocurrent action spectra is limited to ca. 50% with **3a**. The presence of C₁₂ alkoxy chains on the cyclometalated ligand results in an increase of up to 70%, as exemplified by **3b**. Notably, this is lower than what can be obtained when iodine is used as redox mediator. The solar-to-electricity conversion efficiencies were evaluated by recording the J–V characteristics under simulated AM 1.5 G illumination (100 mW cm⁻²). Results are depicted in Figure 4b and photovoltaic parameters are reported in Table 1. As expected, the J_{SC} values follow

Table 1: Detailed photovoltaic parameters of devices employing **3a** and **3b** under simulated AM 1.5 G illumination (100 mW cm^{-2}).

Dye	Electrolyte	J_{SC} [mA cm^{-2}]	V_{OC} [mV]	FF	η [%]
3a	cobalt	8.3	714	0.79	4.7
3b	cobalt	13.2	837	0.78	8.6
3b	iodine	16.3	715	0.75	8.7

the trend observed in IPCE intensities. The measured V_{OC} values show large differences between **3a** and **3b**. The lower V_{OC} obtained with iodine in the case of **3b** highlights the benefit of using a cobalt electrolyte.

Relative shifts in IPCE intensities and *J–V* characteristics can be rationalized based on transient photovoltage decays and charge extraction measurements. While maintaining constant electrolyte, variations in V_{OC} can often be attributed to shifts in the conduction band edge of TiO$_2$.[33] In the presence of $[Co^{II/III}(phen)_3]^{2/3+}$, we observe negligible variation in the conduction band edge (Figure 5a), which indicates
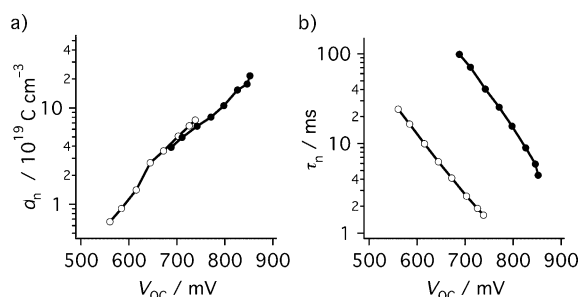
a)   b)

Figure 5. a) Charge density of TiO$_2$ (d_n), and b) electron lifetime (τ_n) against the open-circuit photovoltage (V_{OC}). **3a**+cobalt (○), **3b**+cobalt (●).

that the TiO$_2$ experiences a similar dipole shift with **3a** and **3b**. Therefore, differences in V_{OC} can be attributed to the relative electron lifetimes in TiO$_2$ (τ_n); the electron lifetime of **3b** is prolonged by ca. 1.5 orders of magnitude relative to **3a** (Figure 5b). The recombination of electrons injected into the semiconductor can occur by reductive electron transfer to the electrolyte and/or to the oxidized form of the sensitizer. Given that the time constants for recombination of injected electrons with **3a**$^{·+}$ and **3b**$^{·+}$ are similar, the presence of C$_{12}$ alkoxy chains clearly insulates the TiO$_2$ surface by preventing close proximity with the redox mediator. This effect has a major impact on both the J_{SC} and V_{OC} photovoltaic parameters, as shown in Table 1. Overall, the J_{SC} and V_{OC} obtained for **3a** (8.3 mA cm^{-2} and 714 mV, respectively) contribute to a power conversion efficiency of 4.7%. As a result of the increased electron lifetime, the values measured for **3b** rise to 13.2 mA cm^{-2} and 837 mV, respectively; DSCs with this sensitizer reach efficiencies of up to 8.6% in the presence of a cobalt electrolyte. Notably, this result closely matches that obtained with iodine (8.7%), which has not been thus far reported for a ruthenium(II) sensitizer.

In summary, we have shown that the efficiency of cyclometalated ruthenium(II) sensitizers can be greatly improved in cobalt-based DSCs. Upon increasing the steric properties of the cyclometalating ring, notable improvements in photon-to-current conversion and *J–V* characteristics are observed. Transient absorption decay measurements indicate that the kinetics of recombination and regeneration remain constant, despite the modifications of the sensitizers. However, through charge extraction measurements, the device efficiency is directly correlated to increased surface protection. Physical insulation of the TiO$_2$ surface prolongs the electron lifetime by preventing abnormal recombination of injected electrons into the cobalt(III) species. This approach demonstrates a general principle that leads to unprecedented efficiency for a ruthenium(II) sensitizer used in combination with a cobalt electrolyte.

[1] B. O'Regan, M. Grätzel, *Nature* **1991**, *353*, 737–740.

[2] A. Hagfeldt, G. Boschloo, L. Sun, L. Kloo, H. Pettersson, *Chem. Rev.* **2010**, *110*, 6595–6663.

[3] The V_{OC} is defined as the energy difference between the Fermi level (E_F) of the TiO$_2$ and the HOMO level of the redox mediator, as follows: $V_{OC} = (E_F - E_{HOMO})/e$, where e is the elementary charge.

[4] This equation is applicable under 100 mW cm^{-2} irradiation with J_{SC} in mA cm^{-2} and V_{OC} in V.

[5] M. K. Nazeeruddin, F. De Angelis, S. Fantacci, A. Selloni, G. Viscardi, P. Liska, S. Ito, B. Takeru, M. Grätzel, *J. Am. Chem. Soc.* **2005**, *127*, 16835–16847.

[6] Y. Chiba, A. Islam, Y. Watanabe, R. Komiya, N. Koide, L. Han, *Jpn. J. Appl. Phys.* **2006**, *45*, L638–L640.

[7] F. Gao, Y. Wang, D. Shi, J. Zhang, M. Wang, X. Jing, R. Humphry-Baker, P. Wang, S. M. Zakeeruddin, M. Grätzel, *J. Am. Chem. Soc.* **2008**, *130*, 10720–10728.

[8] C.-Y. Chen, M. Wang, J.-Y. Li, N. Pootrakulchote, L. Alibabaei, C.-H. Ngoc-le, J.-D. Decoppet, J.-H. Tsai, C. Grätzel, C.-G. Wu et al., *ACS Nano* **2009**, *3*, 3103–3109.

[9] Q. Yu, Y. Wang, Z. Yi, N. Zu, J. Zhang, M. Zhang, P. Wang, *ACS Nano* **2010**, *4*, 6032–6038.

[10] A. Yella, H.-W. Lee, H. N. Tsao, C. Yi, A. K. Chandiran, M. K. Nazeeruddin, E. W.-G. Diau, C.-Y. Yeh, S. M. Zakeeruddin, M. Grätzel, *Science* **2011**, *334*, 629–634.

[11] S. A. Sapp, C. M. Elliott, C. Contado, S. Caramori, C. A. Bignozzi, *J. Am. Chem. Soc.* **2002**, *124*, 11215–11222.

[12] S. M. Feldt, E. A. Gibson, E. Gabrielsson, L. Sun, G. Boschloo, A. Hagfeldt, *J. Am. Chem. Soc.* **2010**, *132*, 16714–16724.

[13] S. M. Feldt, G. Wang, G. Boschloo, A. Hagfeldt, *J. Phys. Chem. C* **2011**, *115*, 21500–21507.

[14] J.-H. Yum, E. Baranoff, F. Kessler, T. Moehl, S. Ahmad, T. Bessho, A. Marchioro, E. Ghadiri, J.-E. Moser, C. Yi et al., *Nat. Commun.* **2012**, *3*, 631.

[15] M. K. Kashif, J. C. Axelson, N. W. Duffy, C. M. Forsyth, C. J. Chang, J. R. Long, L. Spiccia, U. Bach, *J. Am. Chem. Soc.* **2012**, *134*, 16646–16653.

[16] H. Nusbaumer, S. M. Zakeeruddin, J.-E. Moser, M. Grätzel, *Chem. Eur. J.* **2003**, *9*, 3756–3763.

[17] B. M. Klahr, T. W. Hamann, *J. Phys. Chem. C* **2009**, *113*, 14040–14045.

[18] Y. Liu, J. R. Jennings, Y. Huang, Q. Wang, S. M. Zakeeruddin, M. Grätzel, *J. Phys. Chem. C* **2011**, *115*, 18847 – 18855.

[19] P. G. Bomben, T. J. Gordon, E. Schott, C. P. Berlinguette, *Angew. Chem.* **2011**, *123*, 10870 – 10873; *Angew. Chem. Int. Ed.* **2011**, *50*, 10682 – 10685.

[20] Y. Xie, T. W. Hamann, *J. Phys. Chem. Lett.* **2013**, *4*, 328 – 332.

[21] S. M. Zakeeruddin, M. K. Nazeeruddin, R. Humphry-Baker, P. Péchy, P. Quagliotto, C. Barolo, G. Viscardi, M. Grätzel, *Langmuir* **2002**, *18*, 952 – 954.

[22] Y. Liu, J. R. Jennings, X. Wang, Q. Wang, *Phys. Chem. Chem. Phys.* **2013**, *15*, 6170 – 6174.

[23] E. Mosconi, J.-H. Yum, F. Kessler, C. J. Gomez-Garcia, C. Zuccaccia, A. Cinti, M. K. Nazeeruddin, M. Grätzel, F. De Angelis, *J. Am. Chem. Soc.* **2012**, *134*, 19438 – 19453.

[24] P. G. Bomben, K. C. D. Robson, P. A. Sedach, C. P. Berlinguette, *Inorg. Chem.* **2009**, *48*, 9631 – 9643.

[25] T. Bessho, E. Yoneda, J.-H. Yum, M. Guglielmi, I. Tavernelli, H. Imai, U. Rothlisberger, M. K. Nazeeruddin, M. Grätzel, *J. Am. Chem. Soc.* **2009**, *131*, 5930 – 5934.

[26] P. G. Bomben, B. D. Koivisto, C. P. Berlinguette, *Inorg. Chem.* **2010**, *49*, 4960 – 4971.

[27] P. G. Bomben, K. D. Thériault, C. P. Berlinguette, *Eur. J. Inorg. Chem.* **2011**, 1806 – 1814.

[28] N. G. Connelly, W. E. Geiger, *Chem. Rev.* **1996**, *96*, 877 – 910.

[29] The vertical ionization corresponds to the energy difference between the cationic and the neutral species at the molecular geometry of the neutral compound; the adiabatic ionization energy corresponds to the energy difference between the optimized cationic and optimized neutral species.

[30] A. Hagfeldt, M. Grätzel, *Chem. Rev.* **1995**, *95*, 49 – 68.

[31] S. Ardo, G. J. Meyer, *Chem. Soc. Rev.* **2009**, *38*, 115 – 164.

[32] A. Y. Anderson, P. R. F. Barnes, J. R. Durrant, B. C. O'Regan, *J. Phys. Chem. C* **2011**, *115*, 2439 – 2447, and references therein.

[33] P. R. F. Barnes, K. Miettunen, X. Li, A. Y. Anderson, T. Bessho, M. Grätzel, B. C. O'Regan, *Adv. Mater.* **2013**, *25*, 1881 – 1922.